Supporting information
for
Faster crystallization during coral skeleton formation correlates with resilience to ocean acidification

Connor A. Schmidt[1], Cayla A. Stifler[1], Emily L. Luffey[1], Benjamin I. Fordyce[1], Asiya Ahmed[1], Gabriela Barreiro Pujol[1], Carolyn P. Breit[1], Sydney S. Davison[1], Connor N. Klaus[1], Isaac J. Koehler[1], Isabelle M. LeCloux[1], Celeo Matute Diaz[1], Catherine M. Nguyen[1], Virginia Quach[1], Jaden S. Sengkhammee[1], Evan J. Walch[1], Max M. Xiong[1], Eric Tambutté[2], Sylvie Tambutté[2], Tali Mass[3], Pupa U.P.A. Gilbert[1,4,5*]

[1] Department of Physics, University of Wisconsin, Madison, WI 53706, USA.

[2] Department of Marine Biology, Centre Scientifique de Monaco, 98000 Monaco, Principality of Monaco.

[3] University of Haifa, Marine Biology Department, Mt. Carmel, Haifa 31905, Israel.

[4] Chemical Sciences Division, Lawrence Berkeley National Laboratory, Berkeley, CA 94720, USA.

[5] Departments of Chemistry, Materials Science and Engineering, and Geoscience, University of Wisconsin, Madison, WI, 53706, USA.

* Corresponding author: pupa@physics.wisc.edu.

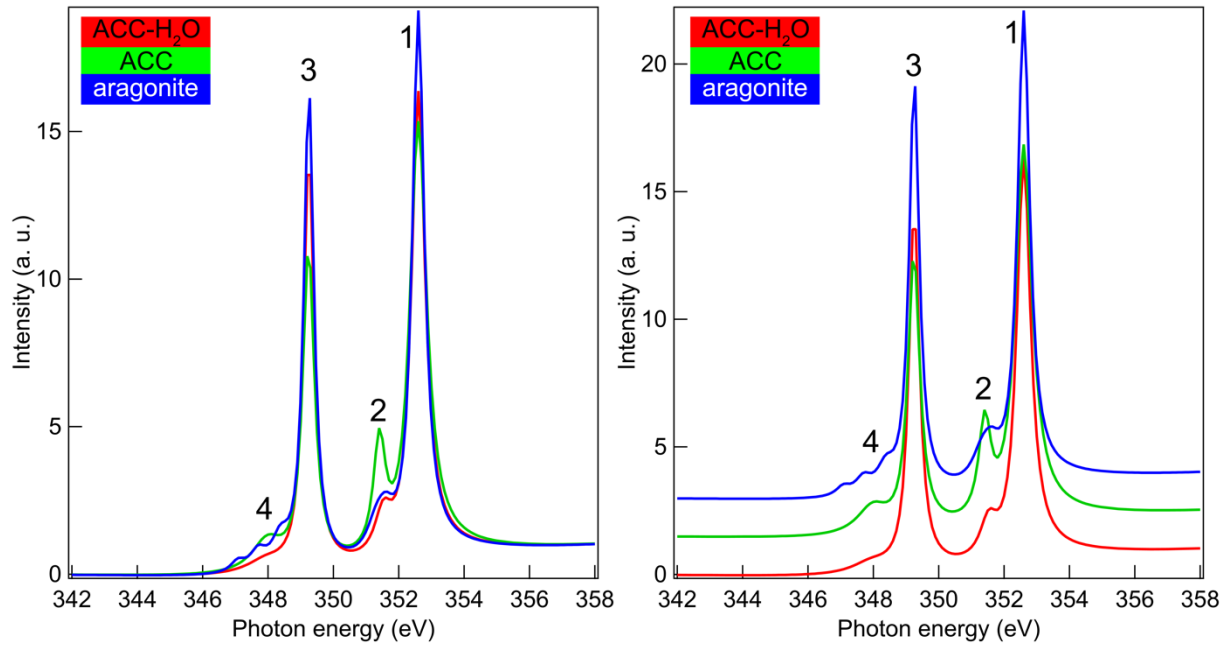

Figure S1. The Cni7 component Ca $L_{2,3}$-edge spectra, used for all component analyses in this work are presented overlapping (left), and displaced vertically for clarity (right). The aragonite spectrum was obtained by extracting 1441 single pixel spectra from 10 Ca movies, from 2 different coral skeletons, aligning them in energy, averaging them, then peak fitting the average. This strategy was used to eliminate any contributions from noise, both statistical (eliminated by peak fitting) and non-statistical (minimized by using spectra from multiple movies). The ACC-H_2O and ACC spectra were extracted from 60 single pixel spectra from 15 Ca movies, all acquired in regenerating sea urchin spines, and previously used as component spectra in Albéric et al. 2019[1]. The 3 spectra were aligned to one another in amplitude and energy between 340 eV and 360 eV, then shifted in energy so the peak 1 was at 352.6 eV, a linear fit to the pre-edge background was subtracted from each of the 3 spectra, and then each spectrum was peak fitted. During peak fitting, 2 arctangents were placed 0.25 eV below peak 3 and peak 1, fixed in position, width, and amplitude, and kept constant for all 3 spectra. Similarly, the background polynomial was fixed and identical for all 3 spectra. These choices were key to obtaining a consistent pre- and post-edge background for all 3 spectra. The results of peak-fitting for the 3 Cni7 component spectra are presented in Table S5. The Cni7 component spectra are included in the Supporting Information as separate .txt files.

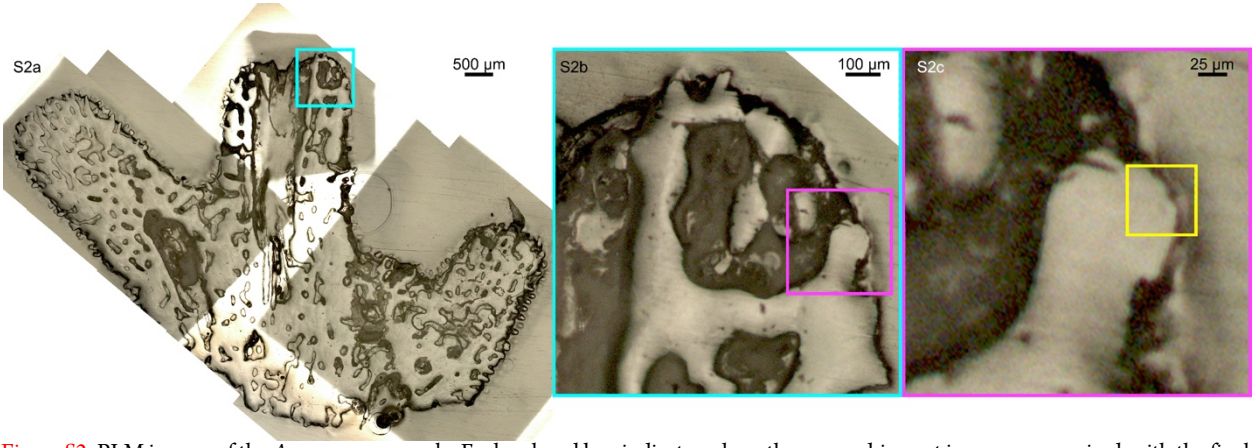

Figure S2. PLM images of the *Acropora* sp. sample. Each colored box indicates where the zoomed-in next image was acquired, with the final yellow box indicating the area of PEEM data acquisition in Figure 2.

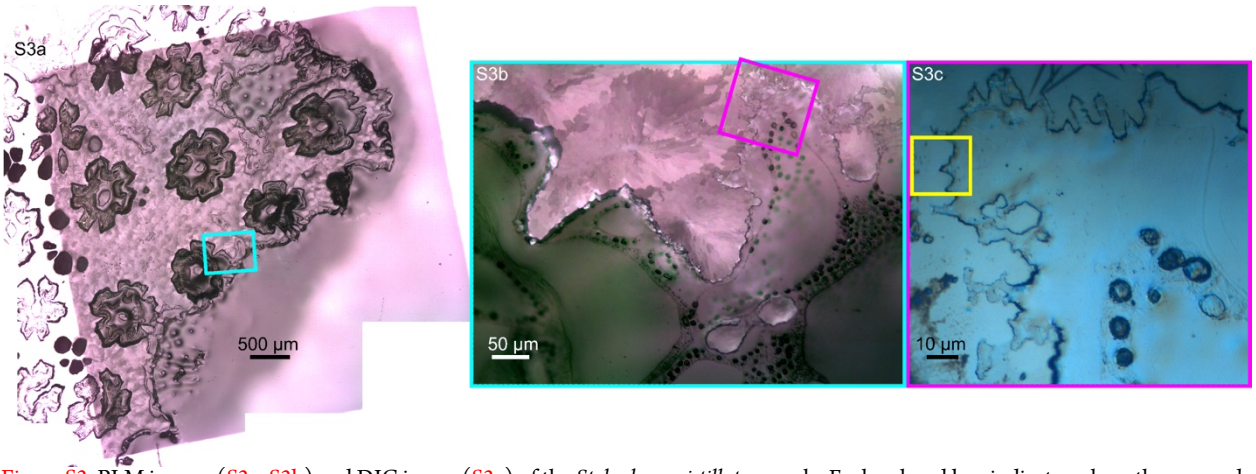

Figure S3. PLM images (S3a, S3b) and DIC image (S3c) of the *Stylophora pistillata* sample. Each colored box indicates where the zoomed-in next image was acquired, with the final yellow box indicating the area of PEEM data acquisition in Figure 3.

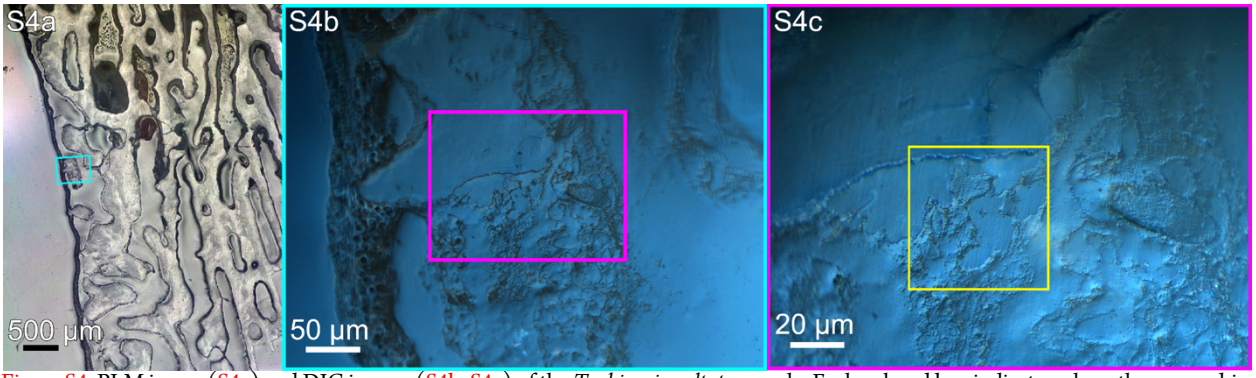

Figure S4. PLM image (S4a) and DIC images (S4b, S4c) of the *Turbinaria peltata* sample. Each colored box indicates where the zoomed-in next image was acquired, with the final yellow box indicating the area of PEEM data acquisition in Figure 4.

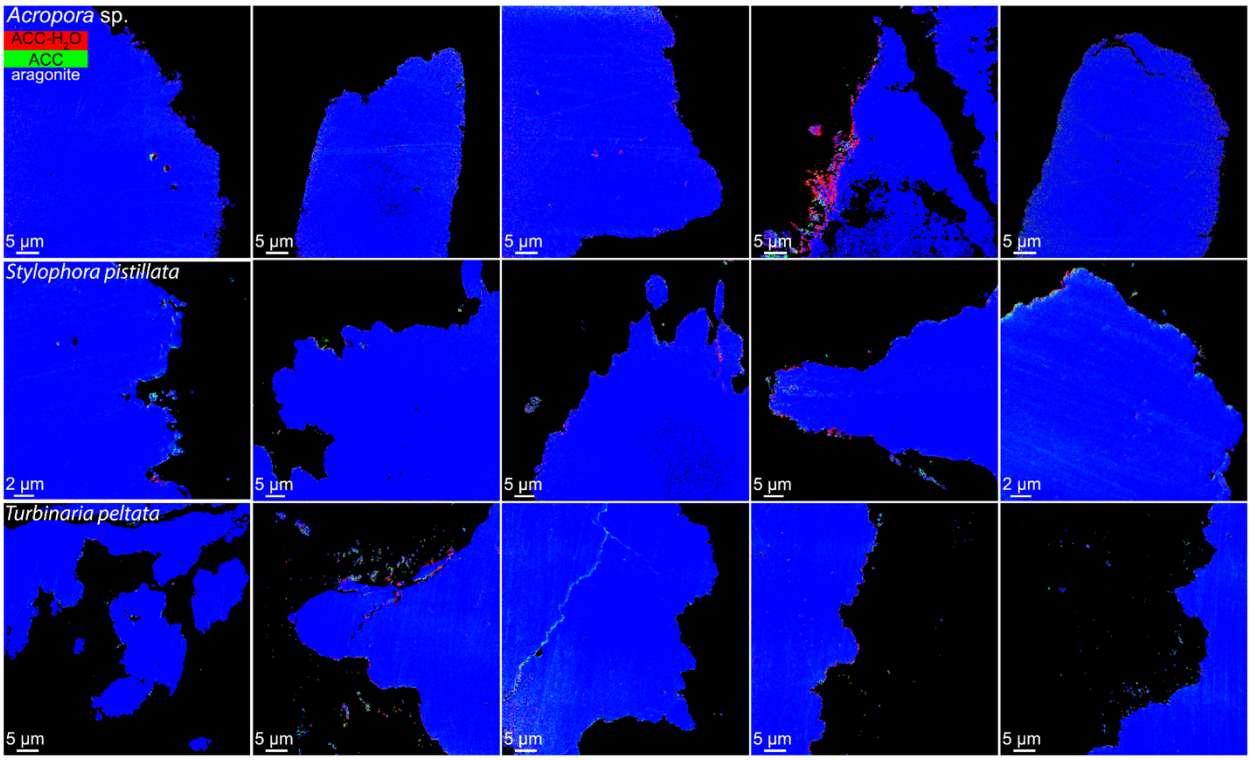

Figure S5. Component maps for each area analyzed in Tables S1-S4, including those shown in Figures 2,3,4 on the left. Five areas from *Acropora*, *Stylophora*, and *Turbinaria* are presented in the top row, the middle, and the bottom row, respectively.

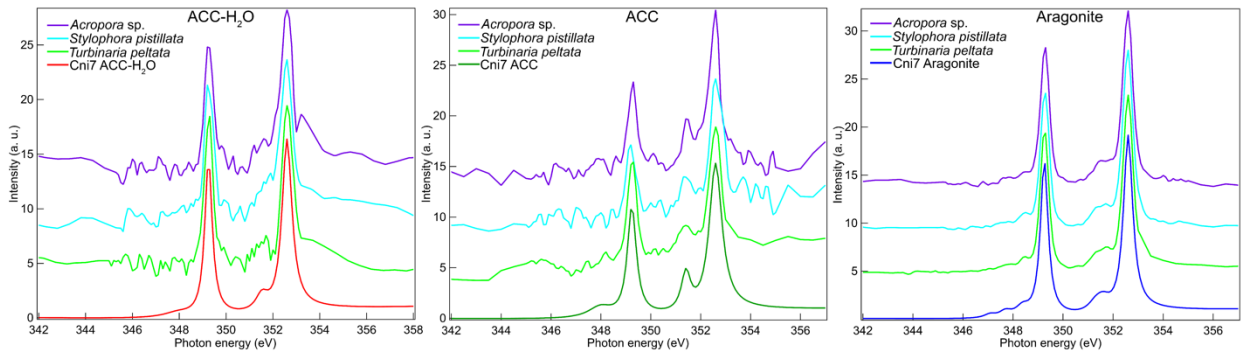

Figure S6. Single-pixel Ca $L_{2,3}$-edge ACC-H_2O, ACC, and aragonite spectra extracted from one of the areas shown in Figures 2,3,4 (top 3 spectra in each panel), and the ACC-H_2O, ACC, and aragonite spectrum from the Cni7 component spectra (bottom spectrum). Pixels are 60 nm for *Acropora* and *Turbinaria* data, 20 nm for *Stylophora* data. The selected single-pixel spectra contained over 90% ACC-H_2O, or ACC, or aragonite, as identified by best-fitting in component mapping. The spectra are displaced vertically for clarity. Spectra from amorphous phases tend to have lower intensity than crystalline ones, leading to spectra with more pronounced noise. This makes sense, as ACC-H_2O has lower Ca density than ACC, and much lower than aragonite.

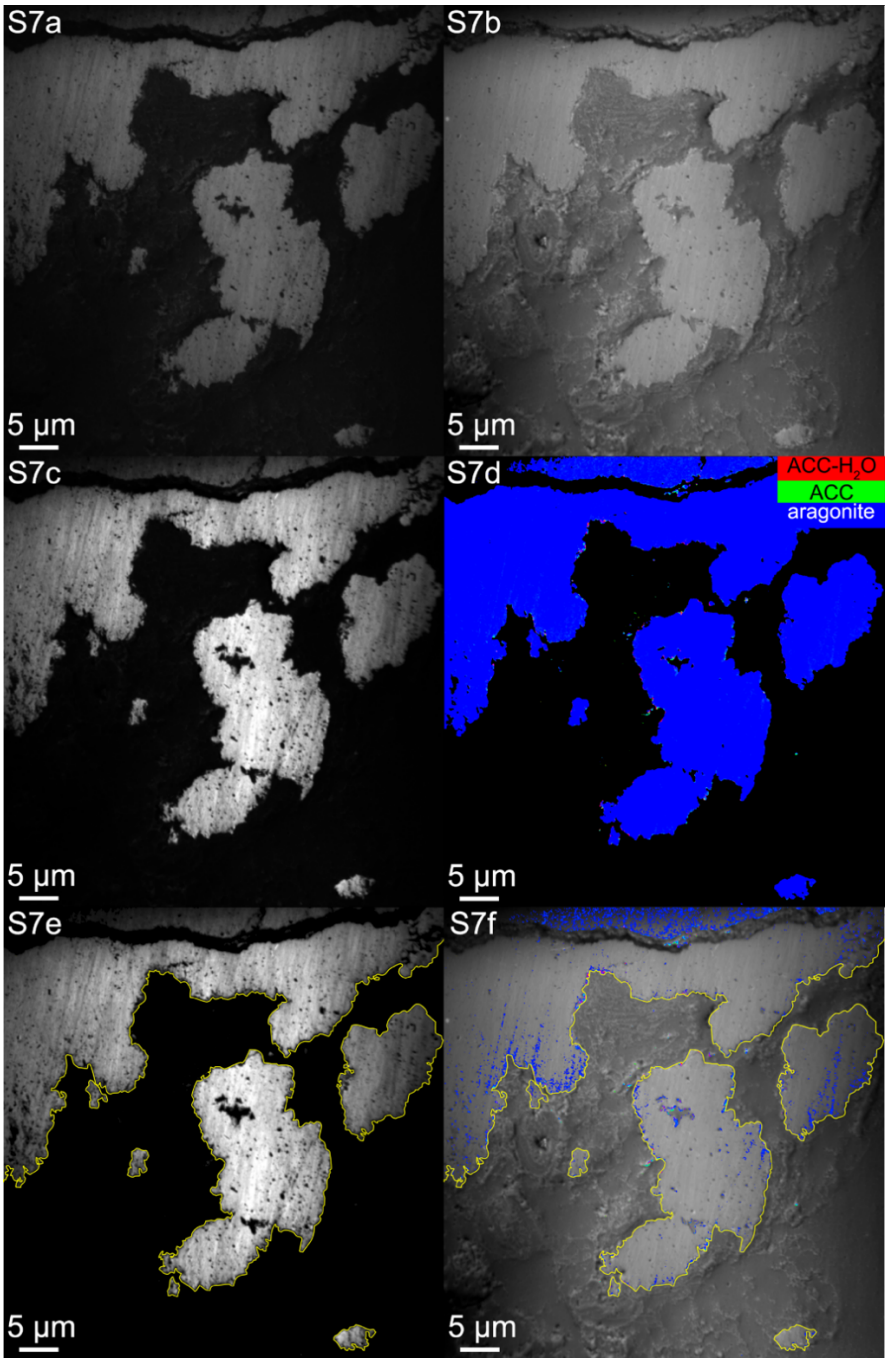

Figure S7. S7a. PEEM single image, taken on peak 1 at 352.6 eV (Fig. S1 shows peak numbers). S7b. Average image, obtained by digitally averaging all 121 PEEM images in a Ca stack. S7c. A Ca concentration map obtained by digital subtraction of images on-peak and off-peak. The on-peak image is the average of 5 images, 1 acquired at the 352.6 eV peak and 4 at ±0.1 and ±0.2 eV from peak, the off-peak image is the average of 9 images acquired at and around 344 eV. S7d. A component map, masked using all 3 masks, the difference mask, the χ^2 mask, and the manual mask eliminating spurious single-pixels in the epoxy or tissue. S7e. The same Ca map in S7c, overlaid with the black mask used in component mapping, and the yellow line outlining the skeleton. The yellow line was produced by outlining the black mask in S7d, in Adobe Photoshop®, using the "stroke" tool, after selecting only the contiguous skeleton and other skeletal regions not connected in this 2D polished cross-section, presumably connected in 3D, and >2 µm. S7f. Average PEEM image, overlaid with the yellow line defined in S7e, and part of the component map in S7d, where all epoxy black pixels and aragonite blue pixels were removed, using the Adobe Photoshop® "magic wand" tool, with a tolerance of 26, to retain all amorphous pixels, and eliminate all crystalline or epoxy pixels. This region's component map, mask, and yellow outline were obtained with precisely the same methods as all others presented in Figures 2d,3d,4d, which are analogous to the panel S7f here.

Table S1

genus	total extra-skeletal volume analyzed (μm^3)	# extra-skeletal particles observed	density of extra-skeletal particles (#particles/μm^3)	average density of extra-skeletal particles	standard deviation
Acropora	5.19	3	0.6	4.0	2.3
	2.43	8	3.3		
	2.62	8	3.1		
	4.53	32	7.1		
	3.98	23	5.8		
Stylophora	0.58	13	22.5	11.9	11.9
	4.22	15	3.6		
	5.46	8	1.5		
	6.93	14	2.0		
	0.47	14	29.8		
Turbinaria	5.31	18	3.4	11.9	10.5
	5.47	160	29.3		
	5.85	40	6.8		
	6.97	128	18.4		
	2.67	4	1.5		

Table S1. **Extra-skeletal particle density.** Results from counting the number of particles observed in each area, divided by the total volume of extra-skeletal space analyzed in each area by PEEM with component mapping. Extra-skeletal particles are defined for this purpose as any group of 4 or more contiguous unmasked pixels outside of the skeleton. Extra-skeletal volume analyzed is obtained by the measuring the number of pixels outside the skeleton, converting that into an area in μm^2, and multiplying it by the 0.003 μm thickness of probed with component mapping. *Stylophora* and *Turbinaria* have areas of high- and low-density of extra-skeletal particles, giving rise to the larger standard deviation measured.

Table S2

genus	total # pixels intra-skeletal, not masked	# ACC-H_2O intra-skeletal pixels	# ACC intra-skeletal pixels	% intra-skeletal amorphous pixels	% intra-skeletal crystalline pixels	average % intra-skeletal amorphous pixels	standard deviation
Acropora	65200	4416	6378	16.6	83.4	23.9	9.2
	93936	8395	19086	29.3	70.7		
	75819	5820	6228	15.9	84.1		
	153553	20980	10230	20.3	79.7		
	110387	13555	27626	37.3	62.7		
Stylophora	151682	2855	11890	9.7	90.3	15.0	6.6
	113654	2768	5481	7.3	92.7		
	99257	6778	9600	16.5	83.5		
	92290	6528	9535	17.4	82.6		
	175832	8103	33889	23.9	76.1		
Turbinaria	190544	1645	4273	3.1	96.9	12.2	5.7
	95267	6065	8989	15.8	84.2		
	79155	1137	7990	11.5	88.5		
	59335	3760	6918	18.0	82.0		
	68317	1201	7419	12.6	87.4		

Table S2. **Intra-skeletal percentages of amorphous pixels.** Results from counting the number of (#) amorphous pixels in the surface 2μm-thick band of all coral areas analyzed. The # pixels were counted in Adobe Photoshop® as described in the Methods. Only pixels with ≥10% of the relevant phase were counted for each amorphous phase. Crystalline pixels were those with >90% aragonite. In the first row of each genus are the data presented in Figures 2,3,4, and in following rows are data from other areas in the genus. Different total pixel counts arise from different fields of view and different amounts of skeletal surface area, so the % amorphous pixels is the most important number. The last two columns show the average % amorphous pixels and the standard deviation for each genus.

Table S3

genus	total # pixels extra-skeletal, not masked	# ACC-H_2O extra-skeletal pixels	# ACC extra-skeletal pixels	% extra-skeletal amorphous pixels	% extra-skeletal crystalline pixels	average % extra-skeletal amorphous pixels ± StDev	average % 1-µm-skeleton surface amorphous pixels ± StDev	significant?
Acropora	1021	192	176	36.0	74.0	63.0 ± 22.8	28.9 ± 10.0	yes p=0.075
	364	93	74	45.9	54.1			
	18977	8095	6865	78.8	21.2			
	1039	388	561	91.3	8.7			
Stylophora	3160	609	1922	80.1	19.9	91.2 ± 8.4	23.7 ± 9.1	yes p=0.0000047
	956	373	636	100	0.0			
	2751	1016	1536	92.8	7.2			
	1698	651	816	86.4	13.6			
	1415	538	749	91.0	9.0			
Turbinaria	700	133	312	63.6	36.4	81.9 ± 11.1	18.8 ± 8.6	yes p=0.00032
	14305	5438	7584	91.0	9.0			
	1533	500	888	90.5	9.5			
	4129	900	2503	82.4	17.6			

Table S3. **Extra-skeletal percentages of amorphous pixels.** Results from counting the number of (#) amorphous pixels in particles outside the skeleton in all coral areas analyzed, except for one area of *Acropora* and one area of *Turbinaria* that did not contain any extra-skeletal particles. As in Table S2, only pixels with ≥10% of the relevant phase were counted for each amorphous phase. Crystalline pixels were those with >90% aragonite. Again, in the first row of each genus are the data presented in Figures 2,3,4, and in following rows are data from other areas in the genus. Again, different total pixel counts arise from different fields of view and different amounts of extra-skeletal particles, so the % amorphous pixels is the most important number. The % of amorphous pixels can be over 100% because ACC and ACC-H_2O are counted separately, thus, if a pixel has both >10% ACC-H_2O >10% ACC it is counted twice. This only occurred in one area, which had 100.6%, and was manually adjusted to 100% amorphous and 0% crystalline, which are physically realistic numbers.

For comparison, in the second to last column we included the % amorphous pixels detected in the outermost 1 µm layer of the skeleton, termed "skeleton surface", which contains the greatest % amorphous pixels compared with any other part of the skeleton. The extra-skeletal particles contain a significantly higher % of amorphous pixels than the most amorphous skeleton surface. The significance and corresponding p-values are indicated in the last column. P-values listed were calculated using a 2-sample t-test, without assuming equal variances.

Table S4

genus	Depth in coral skeleton (µm)	% amorphous pixels in A194	% amorphous pixels in A192	% amorphous pixels in A202	% amorphous pixels in A196	% amorphous pixels in A200	avg % amorphous pixels in 5 areas	standard deviation across 5 areas
Acropora	0.11	33.4	52.0	68.3	37.2	51.9	48.5	13.9
	0.26	27.6	47.8	58.5	30.1	47.2	42.2	13.1
	0.53	24.4	42.4	52.0	24.4	38.6	36.4	12.0
	1	21.3	36.4	45.3	20.3	28.9	30.4	10.6
	2	16.6	29.3	37.3	15.9	20.3	23.9	9.2
	4	12.0	21.7	29.3	12.2	16.3	18.3	7.3
Stylophora	**Depth in coral skeleton (µm)**	**% amorphous pixels in S146**	**% amorphous pixels in S01**	**% amorphous pixels in S11**	**% amorphous pixels in S15**	**% amorphous pixels in S99**	**avg % amorphous pixels in 5 areas**	**standard deviation across 5 areas**
	0.125	31.5	33.4	47.3	58.1	66.2	47.3	15.1
	0.25	29.8	27.4	42.0	50.9	61.8	42.4	14.4
	0.5	24.7	19.1	33.9	40.4	53.1	34.2	13.3
	1	16.9	11.8	24.2	27.5	38.1	23.7	10.2
	2	9.7	7.3	16.5	17.4	23.9	15.0	6.6
	4	5.6	4.8	11.5	11.3	15.7	9.8	4.5
Turbinaria	**Depth in coral skeleton (µm)**	**% amorphous pixels in T35**	**% amorphous pixels in T31**	**% amorphous pixels in T37**	**% amorphous pixels in T61**	**% amorphous pixels in T63**	**avg % amorphous pixels in 5 areas**	**standard deviation across 5 areas**
	0.16	22.9	54.2	32.1	73.6	40.5	44.7	19.8
	0.27	12.8	44.1	33.4	66.3	32.9	37.9	19.5
	0.5	8.5	32.4	24.4	43.3	25.7	26.9	12.7
	1	5.2	22.6	17.3	28.7	18.7	18.5	8.6
	2	3.1	15.9	11.5	18.0	12.6	12.2	5.7
	4	2.2	11.3	8.9	11.5	9.6	8.7	3.8

Table S4. **Intra-skeletal percentages of amorphous pixels vs. distance from surface.** Results from counting the percentage of (%) pixels amorphous pixels (either $ACCH_2O$ or ACC) within the skeleton surface, at various distances from the surface, indicated by a dotted line in Figures 2,3,4. Each genus was measured in quintuplicate, and all data are averaged over the 5 areas in the last column. These data decay logarithmically, as shown in Figure 5.

Table S5

Fit parameters	ACC-H_2O	ACC	Aragonite
p0	**-0.22154**	**-0.22154**	**-0.22154**
p1	**-0.017219**	**-0.017219**	**-0.017219**
p2	**0.0021331**	**0.0021331**	**0.0021331**
p3	**0.00020401**	**0.00020401**	**0.00020401**
pk1 Lorentzian Amplitude	12.411	14.14	12.617
pk1 position	*352.6*	*352.6*	***352.6***
Width	0.51202	0.62488	0.4439
pk2 Lorentzian Amplitude	**1.55**	**2.7**	**1.35**
pk2 position	***351.53***	*351.41*	***351.6***
Width	**0.65**	**0.45**	**0.7**
pk3 Lorentzian Amplitude			**1**
pk2' position			***351.3***
Width			**0.7**
pk4 Lorentzian Amplitude	8.5172	7.2712	9.3555
pk3 position	*349.25*	*349.24*	*349.25*
Width	0.38397	0.4326	0.36859
pk5 Lorentzian Amplitude	1.1156	2.0779	**1**
pk4 position	*347.95*	*347.98*	***348.38***
Width	0.2	1.1895	**0.65**
pk6 Lorentzian Amplitude			**0.6**
pk4' position			***347.7***
Width			**0.6**
pk7 Lorentzian Amplitude			**0.3**
pk4" position			***347.08***
Width			**0.5322**
AT1 Arc-Tangent Amplitude	**0.3**	**0.3**	**0.3**
AT1 position	***349***	***349***	***349***
Width	**0.2**	**0.2**	**0.2**
AT2 Arc-Tangent Amplitude	**0.8**	**0.8**	**0.8**
AT2 position	***352.35***	***352.35***	***352.35***
Width	**0.2**	**0.2**	**0.2**

Table S5. **Component spectra peak-fitting parameters.** Cni7 Fit parameters used in peak-fitting the Cni7 component spectra. Values in **bold** were held, that is, not allowed to change during peak fitting in Igor Pro Carbon® using GG Macros[2]. *Red italics* font indicates energy-positions. Aragonite required the use of several more Lorentzian curves than ACC-H_2O or ACC, so some rows are blank for the amorphous phases. Abbreviations: pk = peak, AT = arctan.

Supporting references

1. Albéric, M.; Stifler, C. A.; Zou, Z.; Sun, C.-Y.; Killian, C. E.; Valencia, S.; Mawass, M.-A.; Bertinetti, L.; Gilbert, P. U. P. A.; Politi, Y., Growth and regrowth of adult sea urchin spines involve hydrated and anhydrous amorphous calcium carbonate precursors. *Journal of Structural Biology: X* **2019,** *1*, 100004.
2. GG–Macros, http://home.physics.wisc.edu/gilbert/software.htm **2021**.